RESEARCH PAPER

Melatonin and breast cancer: a mathematical modeling approach in blind women

Aytekin Enver [iD] 1,*,‡ and **Fatma Ayaz** [iD] 1,‡

1 Department of Mathematics, Gazi University, 06560 Ankara, Türkiye [ROR]

* Corresponding Author
‡ aytekinanwer@gmail.com (Aytekin Enver); fayaz@gazi.edu.tr (Fatma Ayaz)

Abstract

Melatonin, a hormone secreted by the pineal gland, regulates circadian rhythms and exhibits strong anticancer potential through its antioxidant, immunomodulatory, and hormonal effects. This study develops a novel reaction–diffusion mathematical model to describe multiscale interactions among melatonin, breast cancer cells, and immune responses, emphasizing blind women who sustain high melatonin levels due to a lack of light perception. The model uniquely integrates hormonal, oxidative, and immune processes within a unified spatio-temporal framework, enabling joint analysis of tumor proliferation, melatonin-induced inhibition, immune cytotoxicity, and fibroblast-mediated tumor stimulation. Epidemiological evidence indicates that blind women show a markedly lower incidence of hormone-dependent cancers, attributed to continuous melatonin activity. Numerical simulations demonstrate that elevated melatonin concentrations suppress tumor growth, strengthen immune activity, and reduce fibroblast-driven promotion. Moreover, stress-related melatonin depletion is shown to disrupt tumor–immune balance, supporting the hypothesis that circadian rhythm disturbance accelerates tumor progression. The findings offer mechanistic insight into melatonin's dual preventive and therapeutic roles and establish a quantitative link between biochemical regulation and tumor dynamics. By coupling biological data with mathematical rigor, the proposed framework advances mathematical oncology by uniting circadian biology, immunology, and tumor modeling within a single analytical structure.

Keywords: Melatonin; breast cancer; mathematical modeling; reaction-diffusion; blind women

AMS 2020 Classification: 35K57; 35Q92; 92B05; 92C50; 92C37

1 Introduction

The global epidemiological landscape of cancer is systematically monitored through the GLOBO-CAN 2022 database, developed by the International Agency for Research on Cancer (IARC) [1, 2]. This resource provides estimates of incidence and mortality for 36 cancer types across 185 countries, enabling nations to evaluate their current cancer burden, design control strategies, and

define priority areas for intervention. For Türkiye, the GLOBOCAN 2022 data highlight a steadily increasing cancer burden among women, with hormone-dependent tumors playing a particularly dominant role [2, 3].

According to the 2022 estimates, breast cancer accounted for approximately one quarter (23.5%) of all female cancers in Türkiye (see Figure 1 and Figure 2). These figures underscore breast cancer not only as the most frequent malignancy among women but also as one of the most pressing public health issues in the country. Following breast cancer, the most common malignancies were thyroid cancer (11.6%), colorectal (9.3%), lung (7.4%), and corpus uteri cancers (7.3%), reflecting the heterogeneous nature of the female cancer profile and the combined effects of endocrine, metabolic, lifestyle, and environmental factors [4].

In terms of age-standardized incidence rates (ASR, World per 100,000), breast cancer remains by far the leading cancer type, followed by thyroid and colorectal cancers. This distribution emphasizes the necessity of expanding early detection and screening programs such as mammography and colonoscopy, and highlights the importance of further examining hormone-related risk factors. On the other hand, mortality statistics reveal that breast cancer is also the leading cause of cancer-related deaths among women in Türkiye, with lung and colorectal cancers making substantial contributions to overall mortality (see Figure 3). These findings stress the need for differentiated prevention and treatment strategies tailored to distinct tumor types [4].
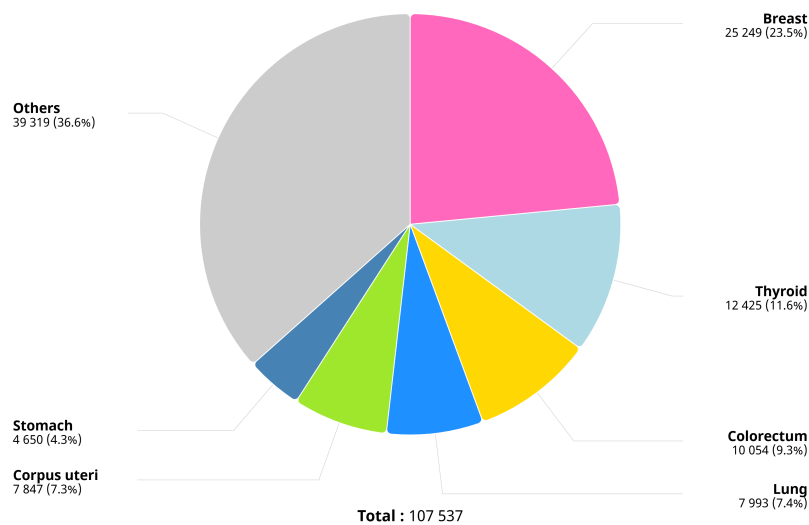
Several mathematical models have been proposed to describe breast cancer progression and hormone-related mechanisms. Reaction–diffusion and ODE-based frameworks have been applied to explore tumor growth, angiogenesis, and treatment dynamics. However, no previous model has incorporated melatonin regulation and immune response simultaneously, particularly in blind populations. The present study fills this gap by introducing a coupled nonlinear reaction–diffusion system integrating these effects.

In conclusion, the GLOBOCAN 2022 data reaffirm the central role of breast cancer in the female cancer burden in Türkiye, while also pointing to the rising importance of thyroid and colorectal malignancies. This epidemiological context provides a critical reference point for mathematical modeling efforts, ensuring that numerical results are interpreted consistently with clinical and biological realities. [2, 5, 6].

This anticipated rise is attributed to population aging, demographic growth, and increased exposure to risk factors such as tobacco use, alcohol consumption, obesity, and environmental pollutants. Hormone-sensitive cancers, such as breast cancer, constitute a significant proportion of these cases. Breast cancer alone accounts for more than 685,000 deaths globally, with substantial regional variations in incidence and mortality. National and international health agencies emphasize the importance of screening programs, particularly mammography, to reduce breast cancer-related mortality. Evidence suggests that initiation of screening at an earlier age, such as 40 years, may substantially decrease mortality, with estimates indicating up to a 40% reduction in breast cancer deaths among women aged 40–74 years when screening is implemented effectively [7]. Participation in screening, however, is shaped by sociodemographic, biological, and psychosocial factors, including education level, comorbidities, lipid metabolism, and psychosocial support. These determinants highlight the importance of multidisciplinary approaches that integrate epidemiology, clinical medicine, and behavioral sciences.

While advances in therapy have improved survival, significant challenges remain, particularly in managing tumor progression driven by oxidative stress, hormonal imbalances, and immune suppression [8]. In this regard, melatonin, a pineal hormone known primarily for its role in regulating circadian rhythms, has attracted significant attention. Beyond its chronobiological functions, melatonin exerts broad-spectrum anticancer effects, including inhibition of tumor growth, modulation of immune responses, and suppression of angiogenesis [9]. Its antioxidative

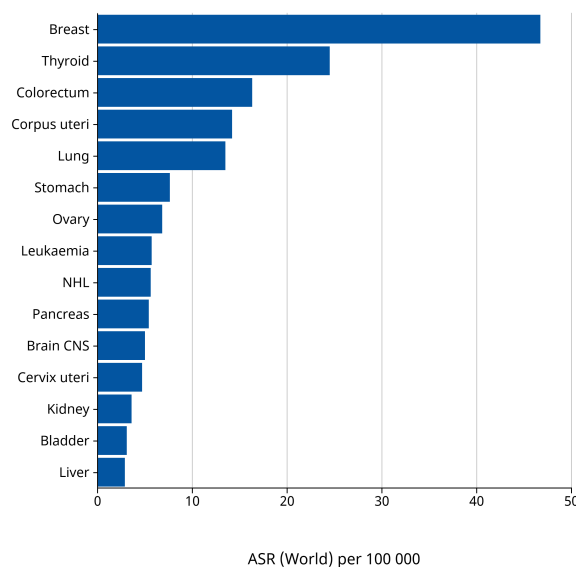**Absolute numbers, Incidence, Females, in 2022**
Türkiye

Figure 1. GLOBOCAN 2022: absolute numbers of female cancer incidence in Türkiye. This figure shows the total counts of diagnosed cases across age groups and cancer types [2]

Age-Standardized Rate (World) per 100 000, Incidence, Females, in 2022
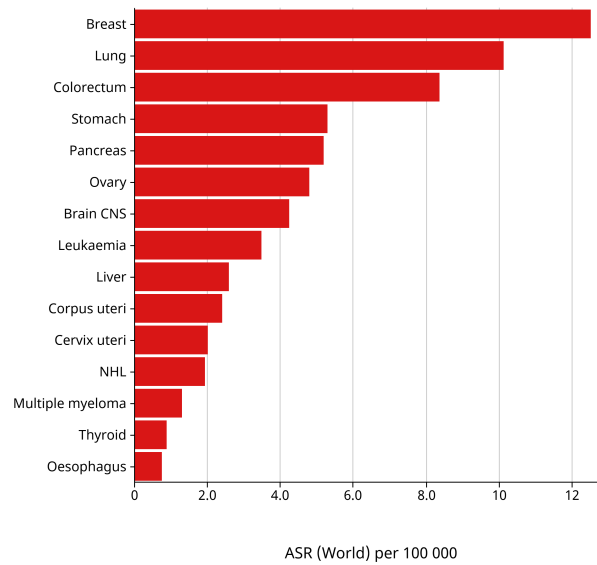Türkiye
(Top 15 cancer sites)

Figure 2. GLOBOCAN 2022: age–standardized (ASR) incidence rates of female cancers in Türkiye. The plot illustrates cancer incidence adjusted for age distribution [2]

properties protect against DNA damage and mutagenesis, while its hormonal regulatory functions counteract estrogen-driven proliferation in hormone-dependent malignancies, especially breast cancer.

Age-Standardized Rate (World) per 100 000, Mortality, Females, in 2022
Türkiye
(Top 15 cancer sites)

Figure 3. GLOBOCAN 2022: age–standardized mortality rates (per 100,000) among females in Türkiye [2]

Epidemiological studies provide further compelling evidence: blind populations, who maintain persistently elevated melatonin levels due to the absence of light-induced suppression, demonstrate a markedly reduced risk of hormone-dependent cancers [10]. This phenomenon underscores melatonin's potential as a preventive and therapeutic agent in breast cancer management. Recent research further suggests that melatonin may enhance responses to immunotherapy and improve outcomes when used as an adjunct to standard treatments [11]. Clinical meta-analyses have confirmed the therapeutic role of melatonin as an adjuvant in cancer treatment, improving patient outcomes and reducing treatment-related toxicity [11].

Given this background, the integration of biological insights with mathematical frameworks provides a powerful approach to understanding the complex dynamics of cancer progression and treatment. In particular, reaction–diffusion models enable the analysis of spatio-temporal interactions between cancer cells, immune components, and therapeutic agents such as melatonin. By capturing the interplay between proliferation, diffusion, and immune modulation, such models offer a promising avenue to explore preventive and therapeutic strategies in breast cancer.

The study is organized as follows: Section 2 presents the biological background related to melatonin and breast cancer mechanisms; Section 3 introduces the mathematical model; Section 4 explains the analytical framework; Section 5 discusses the local stability analysis; Section 6 describes the model parameters; Section 7 provides the numerical solution and simulation results; and Section 8 concludes the study with final remarks and perspectives.

Study objective

The objective of this study is to investigate, through a reaction–diffusion mathematical framework, the regulatory role of melatonin in breast cancer dynamics and its interaction with immune responses. The proposed model aims to capture the spatio–temporal behavior of tumor growth under melatonin influence, integrating biological, biochemical, and physiological mechanisms into a unified mathematical structure. By analyzing both theoretical and numerical aspects, this

study seeks to elucidate how variations in melatonin levels particularly elevated concentrations observed in blind women affect tumor proliferation, immune activation, and system stability.

2 Biological basis: melatonin in cancer and immunomodulation

Mechanisms of action

Antioxidant effects

Melatonin acts as a potent endogenous antioxidant with both direct and indirect mechanisms of action. At the molecular level, melatonin directly scavenges a wide spectrum of reactive oxygen species (ROS), including hydroxyl radicals ($\cdot$OH), superoxide anions (O_2^-), and hydrogen peroxide (H_2O_2). These actions reduce oxidative stress within the tumor microenvironment, a critical driver of oncogenesis, tumor progression, and resistance to therapy. By neutralizing ROS, melatonin prevents oxidative modifications of DNA (Deoxyribonucleic Acid), lipids, and proteins that are commonly implicated in mutagenesis and malignant transformation.

In addition to its direct free radical scavenging, melatonin enhances the endogenous antioxidant defense system by upregulating key enzymes such as superoxide dismutase (SOD), catalase (CAT), and glutathione peroxidase (GPx). This dual protective mechanism provides a sustained defense against redox imbalance, contributing to the stabilization of the cellular genome and reduction of mutation rates in rapidly dividing tumor cells. Furthermore, melatonin's amphiphilic nature enables it to cross cell membranes and mitochondrial compartments, thereby providing protection at critical sites of ROS production, particularly within the electron transport chain.

Emerging evidence also indicates that melatonin interacts with redox-sensitive signaling pathways, such as NF-κB Nuclear Factor kappa-light-chain-enhancer of activated B cells and Nrf2 Nuclear factor erythroid 2–related factor 2, leading to downregulation of pro-oxidant genes and upregulation of cytoprotective transcriptional programs. These regulatory effects link melatonin's antioxidant properties with its ability to modulate immune surveillance and apoptotic signaling cascades, thereby integrating oxidative stress control with tumor suppression. Notably, in hormone-sensitive cancers such as breast carcinoma, melatonin's antioxidant effects intersect with its anti-estrogenic actions, reinforcing its role as a multitargeted agent in both cancer prevention and therapy.

Hormonal modulation

Melatonin exerts profound effects on hormone-dependent cancers through its ability to modulate estrogen metabolism and signaling pathways. One of the principal mechanisms is its inhibitory action on aromatase, the cytochrome P450 enzyme that catalyzes the conversion of androgens to estrogens. By suppressing aromatase activity, melatonin reduces local and systemic estrogen levels, thereby limiting one of the major growth stimuli for estrogen receptor (ER)-positive breast cancers. This mechanism is particularly relevant given that high estrogen exposure is strongly correlated with increased risk of breast carcinogenesis and recurrence.

Beyond regulating estrogen synthesis, melatonin also modulates estrogen responsiveness at the receptor level. It has been shown to downregulate the expression of ERα and ERβ, thereby reducing the sensitivity of breast cancer cells to estrogen-driven proliferation. Through this dual action-lowering estrogen availability and decreasing receptor expression-melatonin acts as a powerful suppressor of estrogen-mediated tumor growth [12]. Importantly, this regulation extends to the tumor microenvironment, where melatonin influences vascular endothelial growth factor (VEGF)-dependent angiogenesis and other paracrine signaling mechanisms that are often amplified in hormone-sensitive cancers.

Another clinically relevant aspect of melatonin's hormonal modulation is its capacity to synergize

with conventional endocrine therapies. Experimental studies indicate that melatonin enhances the efficacy of anti-estrogen drugs such as tamoxifen, a cornerstone in the treatment of ER-positive breast cancer, by augmenting their inhibitory effects on cell cycle progression and survival pathways [11]. This pharmacodynamic interaction suggests that melatonin may function not only as a preventive agent but also as an adjuvant therapy, improving treatment outcomes and potentially reducing resistance to endocrine drugs.

Preclinical studies strongly support this concept. In ER-positive breast cancer models, melatonin has been shown to suppress tumor growth, reduce angiogenic activity, and promote apoptosis of malignant cells [13]. Collectively, these findings emphasize melatonin's unique role as both a regulator of estrogen homeostasis and an enhancer of therapeutic responsiveness, highlighting its translational potential in the management of hormone-sensitive malignancies.

Immune activation

Melatonin plays a pivotal role in regulating immune function by exerting both stimulatory and modulatory effects, ultimately favoring antitumor immunity. Its immunoregulatory actions extend across multiple immune cell populations and cytokine networks, positioning melatonin as a critical component in tumor–immune system interactions.

Enhancing immune cell activity. Melatonin promotes the activation and proliferation of innate and adaptive immune effector cells. Specifically, it enhances the cytotoxic potential of natural killer (NK) cells and cytotoxic T lymphocytes (CTLs), both of which are fundamental in recognizing and destroying malignant cells. Mechanistic studies demonstrate that melatonin upregulates the expression of perforin and granzymes, cytolytic molecules essential for tumor cell apoptosis, thereby boosting the tumor-killing efficacy of NK cells and CTLs. These actions are consistent with melatonin's ability to reinforce immune surveillance during early and advanced stages of cancer.

Suppressing immunosuppressive cells. In addition to enhancing effector immunity, melatonin counteracts the tumor-induced immunosuppressive microenvironment. It reduces the activity of tumor-associated macrophages (TAMs) and regulatory T cells (Tregs), both of which play central roles in dampening antitumor responses and promoting immune evasion. By suppressing these populations, melatonin shifts the immune balance towards a pro-inflammatory, tumor-inhibiting state. Such modulation is particularly relevant in the context of modern immunotherapies, where overcoming immune suppression is a major therapeutic challenge.

Cytokine modulation. Melatonin also exerts a profound impact on cytokine networks. It promotes the secretion of antitumor cytokines, notably interferon-gamma (IFN-γ), while reducing the levels of immunosuppressive and tumor-promoting cytokines such as transforming growth factor-beta (TGF-β) and interleukin-10 (IL-10). This cytokine shift enhances effector T cell and NK cell activity while simultaneously limiting the chronic inflammatory milieu that fosters tumor progression. Collectively, these immunomodulatory properties indicate that melatonin not only enhances intrinsic antitumor immunity but also may synergize with checkpoint inhibitors and other immune-based therapies, highlighting its translational potential in cancer immuno-oncology.

Insights from blind populations

Epidemiological studies have consistently reported a markedly reduced incidence of hormone-dependent cancers, particularly breast cancer, among blind individuals [14]. This protective association has been attributed primarily to their persistently elevated nocturnal melatonin levels,

which are maintained in the absence of light perception. Unlike sighted individuals, in whom exposure to natural or artificial light at night suppresses pineal melatonin secretion, blind individuals demonstrate robust circadian melatonin rhythms [8]. This stable secretion profile is thought to preserve the anticarcinogenic effects of melatonin, including its antioxidative, anti-estrogenic, and immunomodulatory actions.

Cancer risk reduction in blind women. Large cohort studies, such as the investigation conducted by Pukkala et al., revealed that blind women exhibit up to a 50% lower risk of developing breast cancer compared with their sighted counterparts [14]. The magnitude of this protective effect underscores the biological plausibility that persistent melatonin exposure exerts significant preventive benefits. Mechanistically, elevated melatonin reduces estrogen synthesis via aromatase inhibition, downregulates estrogen receptor signaling, and simultaneously protects cellular DNA from oxidative damage through radical scavenging pathways. Together, these effects establish a durable barrier against carcinogenesis in hormone-sensitive tissues [15].

Implications for circadian disruption in sighted populations. The reduced cancer incidence among blind individuals also provides critical insight into the carcinogenic potential of circadian disruption. Epidemiological studies link such disruption to increased risks of breast, prostate, and other hormone-dependent cancers. In contrast, the epidemiological resilience of blind populations highlights the importance of uninterrupted melatonin signaling as a natural defense against tumorigenesis [10]. This comparison strengthens the rationale for considering melatonin supplementation or circadian-protective interventions as preventive and therapeutic strategies, especially in at-risk populations such as shift workers.

Overall, the biological and clinical insights gained from blind populations emphasize the pivotal role of melatonin in maintaining hormonal balance, limiting oxidative stress, and sustaining immune surveillance. These findings not only advance our understanding of melatonin's protective mechanisms but also open new avenues for its application in circadian oncology and cancer prevention.

3 Mathematical model: reaction-diffusion framework

To investigate the interplay between cancer cells, melatonin, and immune components in the tumor microenvironment, we employ a reaction–diffusion framework. This class of models is particularly suitable for capturing spatiotemporal phenomena, where both local reaction kinetics (cell proliferation, immune activation, hormone signaling) and spatial diffusion (cell migration, molecular transport) shape the overall system dynamics. By integrating biological realism with mathematical rigor, the corresponding system of partial differential equations is presented in the points below, describing tumor growth under melatonin-mediated regulation.

Cancer cell dynamics

The temporal and spatial evolution of cancer cell density $C(x,t)$ is described by

$$\frac{\partial C}{\partial t} = D_C \nabla^2 C + rC\left(1 - \frac{C}{K}\right) - \alpha MC - \beta IC + \varepsilon FC, \tag{1}$$

where D_C represents the diffusion coefficient associated with random motility of tumor cells, r is the intrinsic proliferation rate, and K denotes the local carrying capacity. The logistic growth term $rC(1 - C/K)$ captures density-dependent proliferation, consistent with classical tumor growth models.

The inhibitory influence of melatonin on cancer cells is modeled through the interaction term $-\alpha MC$, reflecting its anti-proliferative and pro-apoptotic properties. Similarly, Ucar et al. [16] immune-mediated cytotoxicity is incorporated via $-\beta IC$, representing direct killing by natural killer (NK) cells and cytotoxic T lymphocytes. Conversely, the contribution of fibroblasts in promoting tumor invasion and extracellular matrix remodeling is modeled by the supportive term $+\varepsilon FC$. Together, these mechanisms provide a balanced view of proliferative and suppressive forces regulating cancer cell dynamics. Recent studies have further elucidated the impact of fibroblast activity and macrophage interactions within tumor microenvironments. The disturbance effect in intracellular calcium dynamics of fibroblast cells using an exponential kernel law, demonstrating that calcium signaling disturbances significantly alter fibroblast proliferation and stress response. Similarly, developed a stochastic tumor modeling framework incorporating macrophages, showing that macrophage-mediated immune interactions play a crucial role in tumor progression and suppression balance. These studies support the biological assumptions adopted in our model regarding fibroblast–tumor coupling and macrophage-driven immune modulation.

Melatonin dynamics

The spatiotemporal distribution of melatonin $M(x,t)$ in the tumor environment evolves according to

$$\frac{\partial M}{\partial t} = D_M \nabla^2 M - \gamma M + p - \rho CM, \tag{2}$$

where D_M denotes the diffusion coefficient describing melatonin transport across tissues, and γ is the natural decay rate. The constant production term p accounts for systemic pineal secretion and local synthesis by immune and stromal cells.

The consumption term $-\rho CM$ represents degradation or neutralization of melatonin by cancer cells, consistent with experimental evidence showing altered melatonin metabolism in malignant tissues. This antagonistic relationship reflects the ability of tumors to diminish melatonin's protective functions, thereby creating a permissive environment for further proliferation. Importantly, this equation captures both systemic rhythmic regulation and localized tumor-associated perturbations in melatonin availability.

Immune cell dynamics

The density of immune effector cells $I(x,t)$ is modeled by

$$\frac{\partial I}{\partial t} = D_I \nabla^2 I + s + \delta MI - \mu CI, \tag{3}$$

where D_I is the diffusion coefficient representing immune cell migration, and s is a baseline source term accounting for recruitment from the bloodstream and lymphoid tissues. The term $+\delta MI$ models melatonin-driven immune stimulation, reflecting enhanced activation and proliferation of NK cells and cytotoxic T cells in the presence of elevated melatonin levels.

The interaction term $-\mu CI$ accounts for tumor-induced immune suppression, a hallmark of cancer progression whereby malignant cells evade immune detection through inhibitory ligands, secretion of immunosuppressive cytokines, and induction of regulatory immune subsets. This formulation ensures that the delicate balance between immune activation and tumor-driven suppression is mathematically represented.

Model significance

The coupled system of Eqs. (1), (2) and (3) integrates the essential biological processes governing tumor growth under melatonin regulation:

- Cancer proliferation constrained by logistic growth, immune-mediated killing, and hormonal suppression,
- Melatonin dynamics incorporating production, degradation, and tumor-associated consumption,
- Immune cell behavior shaped by recruitment, activation via melatonin, and suppression by cancer cells.

This framework provides a foundation for theoretical analysis (e.g., steady states, stability conditions, traveling wave solutions) as well as numerical simulations (e.g., finite difference or finite element approximations). It also allows for parameter exploration to assess therapeutic strategies such as melatonin supplementation, immunotherapy, and stromal-targeted interventions. By bridging biology and mathematics, the model offers valuable insights into how circadian-regulated molecules, such as melatonin, modulate the tumor-immune ecosystem (systematically illustrated in Figure 4).

Initial positivity assumption. We assume that all initial data of the system, including tumor cell density, immune cell concentration, melatonin level, and fibroblast density, are nonnegative and sufficiently smooth functions defined on the spatial domain Ω. That is, for all $x \in \Omega$,

$$u_i(x, 0) \geq 0, \quad \text{for each variable } u_i \in \{C, I, M, F\}.$$

This assumption reflects the biological reality that all measurable quantities represent physical densities or concentrations and must therefore remain positive.

4 Existence and uniqueness proof for the reaction-diffusion system

In this section, we establish the existence of weak solutions for the proposed nonlinear reaction–diffusion system modeling the interactions between cancer cells, melatonin, and immune cells. The proof is constructed using Galerkin approximation, energy estimates, and compactness arguments within Sobolev spaces.

Theorem 1 (Existence of weak solutions for the nonlinear reaction–diffusion system) *Let $\Omega \subset \mathbb{R}^n$ be a bounded domain with smooth boundary $\partial\Omega$. Consider the system*

$$\frac{\partial C}{\partial t} = D_C \nabla^2 C + rC \left(1 - \frac{C}{K}\right) - \alpha MC - \beta IC + \varepsilon FC,$$

$$\frac{\partial M}{\partial t} = D_M \nabla^2 M - \gamma M + p - \rho CM, \tag{4}$$

$$\frac{\partial I}{\partial t} = D_I \nabla^2 I + s + \delta MI - \mu CI,$$

with initial conditions $C(x, 0), M(x, 0), I(x, 0) \in L^2(\Omega)$ and either homogeneous Neumann boundary conditions

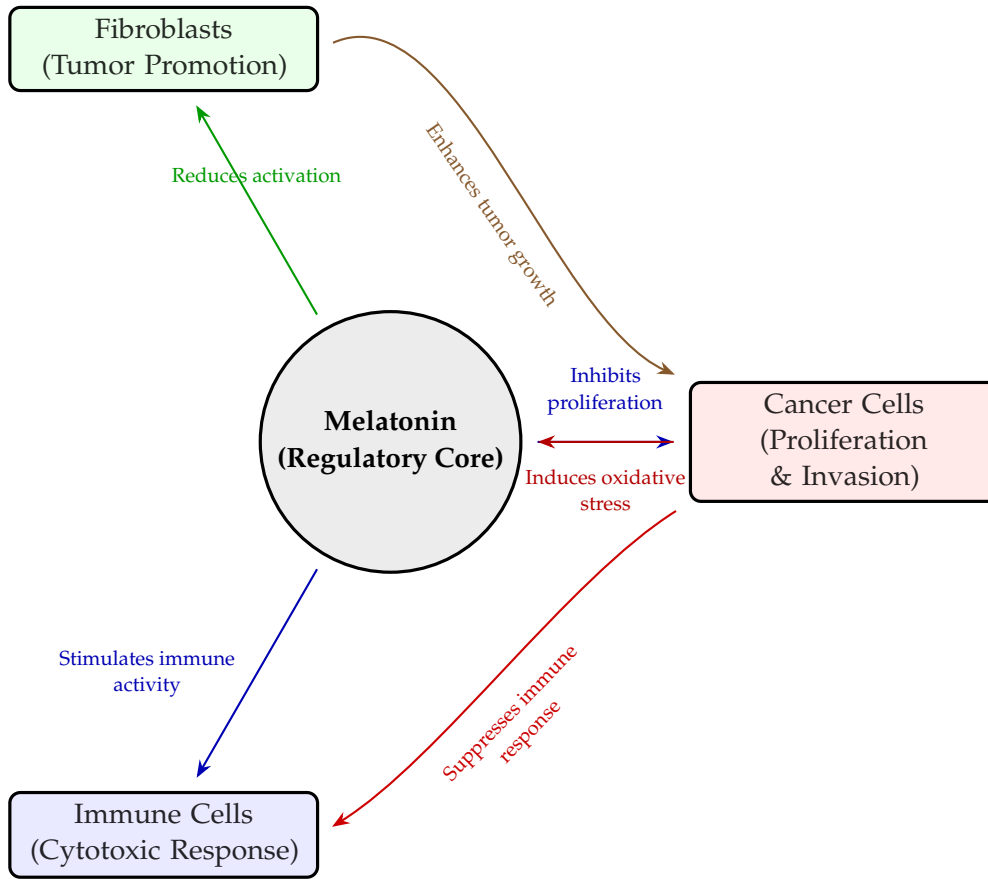$$\nabla C \cdot n = \nabla M \cdot n = \nabla I \cdot n = 0, \quad on \quad \partial\Omega,$$

Figure 4. Schematic representation of melatonin-centered regulatory interactions. Melatonin acts as a central modulator influencing cancer cells, immune dynamics, and fibroblast activity. Blue and green arrows denote inhibitory or regulatory pathways, whereas red and brown arrows indicate pro-tumorigenic feedback and cross-activation mechanisms among peripheral components

or Dirichlet boundary conditions. Assume that all coefficients

$$D_C, D_M, D_I, r, \alpha, \beta, \gamma, \rho, \delta, \mu, \varepsilon, K, s, p > 0.$$

Then there exists at least one nonnegative weak solution

$$(C, M, I) \in L^2\big(0, T; H^1(\Omega)\big), \quad \forall T > 0.$$

Proof We outline the proof in several steps.

Weak formulation. For test functions $\varphi_C, \varphi_M, \varphi_I \in H^1(\Omega)$, multiplying each PDE and integrating over Ω yields:

$$\int_\Omega \frac{\partial C}{\partial t} \varphi_C \, dx + D_C \int_\Omega \nabla C \cdot \nabla \varphi_C \, dx = \int_\Omega \left(rC \left(1 - \frac{C}{K} \right) - \alpha MC - \beta IC + \varepsilon FC \right) \varphi_C \, dx,$$

$$\int_\Omega \frac{\partial M}{\partial t} \varphi_M \, dx + D_M \int_\Omega \nabla M \cdot \nabla \varphi_M \, dx = \int_\Omega (-\gamma M + p - \rho CM) \varphi_M \, dx,$$

$$\int_\Omega \frac{\partial I}{\partial t} \varphi_I \, dx + D_I \int_\Omega \nabla I \cdot \nabla \varphi_I \, dx = \int_\Omega (s + \delta MI - \mu CI) \varphi_I \, dx.$$

This variational formulation ensures the problem is well-posed in $H^1(\Omega)$.

Galerkin approximation. Choose a finite-dimensional subspace $V_n \subset H^1(\Omega)$ with orthonormal basis $\{\varphi_1, \ldots, \varphi_n\}$. Define approximate solutions

$$C_n(x,t) = \sum_{j=1}^{n} c_j(t)\varphi_j(x), \quad M_n(x,t) = \sum_{j=1}^{n} m_j(t)\varphi_j(x), \quad I_n(x,t) = \sum_{j=1}^{n} i_j(t)\varphi_j(x).$$

Substitution into the weak form yields a system of ODEs for coefficients $c_j(t), m_j(t), i_j(t)$, which is locally well-posed.

Energy estimates. Define the energy functional

$$E(t) = \frac{1}{2} \int_\Omega \left(C_n^2 + M_n^2 + I_n^2 \right) dx.$$

Differentiating and applying the weak forms, we obtain

$$\frac{dE}{dt} + \int_\Omega \left(D_C |\nabla C_n|^2 + D_M |\nabla M_n|^2 + D_I |\nabla I_n|^2 \right) dx \leq C\, E(t),$$

for some constant $C > 0$. By Gronwall's inequality, $E(t)$ remains uniformly bounded.

Compactness and convergence. The bounds imply

$$\|C_n\|_{L^\infty(0,T;H^1(\Omega))}^2 + \|M_n\|_{L^\infty(0,T;H^1(\Omega))}^2 + \|I_n\|_{L^\infty(0,T;H^1(\Omega))}^2 \leq C,$$

independent of n. By the Banach–Alaoglu theorem, there exist subsequences converging weakly in $H^1(\Omega)$. To handle nonlinearities, we apply the Aubin–Lions lemma: boundedness in $L^2(0,T;H^1(\Omega))$ and boundedness of time derivatives in $L^2(0,T;H^{-1}(\Omega))$ yield strong convergence in $L^2(0,T;L^2(\Omega))$.

Passage to the limit. Weak convergence handles linear terms, while strong convergence ensures passage to the limit in nonlinear terms such as C^2, MC, and IC. For instance,

$$\int_\Omega rC_n \left(1 - \frac{C_n}{K} \right) \varphi_C dx \to \int_\Omega rC \left(1 - \frac{C}{K} \right) \varphi_C dx.$$

Similar arguments apply for melatonin and immune equations. Thus, the limit functions (C, M, I) satisfy the original weak formulation.

We conclude that there exists at least one weak solution

$$(C, M, I) \in L^2(0,T;H^1(\Omega)), \quad \forall T > 0,$$

to the nonlinear reaction–diffusion system (4).

Theorem 2 (Uniqueness of solutions for the nonlinear reaction–diffusion system) *Let $\Omega \subset \mathbb{R}^n$ be bounded with smooth boundary $\partial\Omega$. Assume all coefficients $D_C, D_M, D_I, r, \alpha, \beta, \gamma, \rho, \delta, \mu, \varepsilon, K, s, p > 0$ are constants.*

Let (C_1, M_1, I_1) and (C_2, M_2, I_2) be two weak solutions to the system (4.1)–(4.3) on $[0, T]$, under the same **nonnegative initial data**

$$C_1(\cdot, 0) = C_2(\cdot, 0), \quad M_1(\cdot, 0) = M_2(\cdot, 0), \quad I_1(\cdot, 0) = I_2(\cdot, 0) \quad in \ L^2(\Omega, \mathbb{R}^3_+),$$

and either homogeneous Neumann or Dirichlet boundary conditions. Suppose moreover that the reaction mapping

$$\mathcal{F}(C, M, I) = \left(rC(1 - \tfrac{C}{K}) - \alpha MC - \beta IC + \varepsilon FC, \ -\gamma M + p - \rho CM, \ s + \delta MI - \mu CI \right),$$

is (locally) Lipschitz on bounded sets of $\mathbb{R}^3$. Then $(C_1, M_1, I_1) = (C_2, M_2, I_2)$ almost everywhere in $\Omega \times [0, T]$.

Proof Set the differences $v_C = C_1 - C_2$, $v_M = M_1 - M_2$, $v_I = I_1 - I_2$, and $v = (v_C, v_M, v_I)$. Subtracting the two systems yields, in $\Omega \times (0, T)$,

$$\partial_t v_C - D_C \Delta v_C = r\left(C_1 - \tfrac{C_1^2}{K} - C_2 + \tfrac{C_2^2}{K}\right) - \alpha(M_1 C_1 - M_2 C_2) - \beta(I_1 C_1 - I_2 C_2) + \varepsilon F v_C,$$
$$\partial_t v_M - D_M \Delta v_M = -\gamma v_M - \rho\left(C_1 M_1 - C_2 M_2\right),$$
$$\partial_t v_I - D_I \Delta v_I = \delta\left(M_1 I_1 - M_2 I_2\right) - \mu\left(C_1 I_1 - C_2 I_2\right),$$

with the same homogeneous boundary conditions as the original system and the zero initial data $v_C(\cdot, 0) = v_M(\cdot, 0) = v_I(\cdot, 0) = 0$ in $L^2(\Omega)$.

Test the three equations by v_C, v_M, v_I respectively and integrate over Ω. Boundary terms vanish by the boundary conditions, giving

$$\frac{1}{2}\frac{d}{dt}\|v_C\|_{L^2}^2 + D_C\|\nabla v_C\|_{L^2}^2 = \int_\Omega \left[r\left(C_1 - \tfrac{C_1^2}{K} - C_2 + \tfrac{C_2^2}{K}\right) - \alpha(M_1 C_1 - M_2 C_2) \right.$$
$$\left. - \beta(I_1 C_1 - I_2 C_2) + \varepsilon F v_C \right] v_C \, dx,$$

$$\frac{1}{2}\frac{d}{dt}\|v_M\|_{L^2}^2 + D_M\|\nabla v_M\|_{L^2}^2 = \int_\Omega \left(-\gamma v_M - \rho(C_1 M_1 - C_2 M_2) \right) v_M \, dx,$$

$$\frac{1}{2}\frac{d}{dt}\|v_I\|_{L^2}^2 + D_I\|\nabla v_I\|_{L^2}^2 = \int_\Omega \left(\delta(M_1 I_1 - M_2 I_2) - \mu(C_1 I_1 - C_2 I_2) \right) v_I \, dx.$$

Rewrite the nonlinear differences, e.g. $C_1 - \tfrac{C_1^2}{K} - C_2 + \tfrac{C_2^2}{K} = v_C\left(1 - \tfrac{C_1 + C_2}{K}\right)$, $M_1 C_1 - M_2 C_2 = M_1 v_C + v_M C_2$, $I_1 C_1 - I_2 C_2 = I_1 v_C + v_I C_2$, $C_1 M_1 - C_2 M_2 = C_1 v_M + v_C M_2$, $M_1 I_1 - M_2 I_2 = M_1 v_I + v_M I_2$. Using Cauchy–Schwarz and Young's inequalities,

$$ab \le \frac{\eta}{2}a^2 + \frac{1}{2\eta}b^2 \qquad (\eta > 0),$$

and the local Lipschitz continuity of $\mathcal{F}$ on bounded sets together with a priori bounds for (C_j, M_j, I_j) from the existence theory, we obtain constants $K_1, K_2 > 0$ (depending on coefficients and L^∞-bounds of the solutions on $[0, T]$) such that

$$\frac{d}{dt}E(t) + \lambda\, \Phi(t) \ \le \ K_1\, E(t),$$

where

$$E(t) = \tfrac{1}{2}\left(\|v_C\|_{L^2}^2 + \|v_M\|_{L^2}^2 + \|v_I\|_{L^2}^2\right), \quad \Phi(t) = \|\nabla v_C\|_{L^2}^2 + \|\nabla v_M\|_{L^2}^2 + \|\nabla v_I\|_{L^2}^2,$$

and $\lambda = \min\{D_C, D_M, D_I\} > 0$. Discarding the nonnegative $\Phi(t)$ term yields

$$\frac{d}{dt}E(t) \leq K_1 E(t).$$

Since $E(0) = 0$ (identical initial data), Gronwall's inequality implies $E(t) = 0$ for all $t \in [0, T]$. Hence $v_C = v_M = v_I = 0$ a.e. in $\Omega \times [0, T]$, i.e. $(C_1, M_1, I_1) = (C_2, M_2, I_2)$ a.e.

Positivity of solutions. Given nonnegative initial conditions and a quasi-positive reaction vector field, the solutions of the reaction–diffusion system remain nonnegative for all $t > 0$. Formally, if $u_i(x, 0) \geq 0$ for all $x \in \Omega$ and each component u_i, then

$$u_i(x, t) \geq 0, \quad \forall (x, t) \in \Omega \times (0, T].$$

This property follows from the maximum principle applied to the reaction–diffusion operator and guarantees that the model is biologically consistent.

5 Local stability analysis of the reaction-diffusion cancer-stress model

We investigate the local stability of a nonlinear reaction–diffusion system that describes the spatio–temporal interactions between cancer cells $C(x, t)$, melatonin $M(x, t)$, and immune response $I(x, t)$ in the presence of chronic stress. The model is defined on a bounded and sufficiently smooth spatial domain $\Omega \subset \mathbb{R}^n$ with outward unit normal vector n, subject to homogeneous Neumann (no–flux) boundary conditions:

$$\nabla C \cdot n = \nabla M \cdot n = \nabla I \cdot n = 0, \qquad x \in \partial\Omega, \ t > 0,$$

which reflect biological impermeability at the tissue boundary.

The governing equations are given by the coupled nonlinear reaction–diffusion system:

$$\frac{\partial C}{\partial t} = D_C \Delta C + rC\left(1 - \frac{C}{K}\right) - \alpha MC - \beta IC + \varepsilon FC, \tag{5}$$

$$\frac{\partial M}{\partial t} = D_M \Delta M - \gamma M + p - \rho CM, \tag{6}$$

$$\frac{\partial I}{\partial t} = D_I \Delta I + s + \delta MI - \mu CI. \tag{7}$$

Eqs. (5)-(7) capture the essential feedback loops between cancer proliferation, circadian regulation by melatonin, and immune activation under chronic stress conditions:

i. Cancer cells grow logistically with intrinsic rate r and carrying capacity K, but are suppressed by melatonin ($-\alpha MC$) and immune responses ($-\beta IC$). The stress term εFC introduces external

stress–induced enhancement of cancer progression.

ii. Melatonin diffuses, decays at rate γ, and is suppressed by cancer cells via $-\rho CM$. Its baseline production is modeled by the constant source p.

iii. Immune cells diffuse, are activated by melatonin through δMI, and are suppressed by cancer cells via $-\mu CI$, while maintaining a baseline input s.

This framework allows the study of how stress, through modulation of melatonin and immune interactions, affects the stability of the tumor microenvironment. In the following subsections, we analyze equilibria of (5)-(7), linearize the system around steady states, and derive local stability criteria in terms of the system parameters.

Steady state and its local stability

We denote the biologically relevant positive steady state by

$$(C^*, M^*, I^*),$$

which satisfies the algebraic system obtained by setting the time derivatives in (5)-(7) equal to zero:

$$0 = rC^*\left(1 - \frac{C^*}{K}\right) - \alpha M^* C^* - \beta I^* C^* + \varepsilon F C^*, \tag{8}$$

$$0 = -\gamma M^* + p - \rho C^* M^*, \tag{9}$$

$$0 = s + \delta M^* I^* - \mu C^* I^*. \tag{10}$$

Eq. (8) represents the balance of cancer proliferation, inhibition by melatonin and immune cells, and stress–induced amplification. Eq. (9) reflects the equilibrium between melatonin production, decay, and suppression by cancer cells. Eq. (10) describes the steady immune response maintained by the baseline source s, activated by melatonin and suppressed by cancer.

To investigate the local stability of (C^*, M^*, I^*), we linearize the system around this equilibrium. Let small perturbations be denoted as

$$C(x, t) = C^* + \widetilde{C}(x, t), \quad M(x, t) = M^* + \widetilde{M}(x, t), \quad I(x, t) = I^* + \widetilde{I}(x, t),$$

where $\widetilde{C}, \widetilde{M}, \widetilde{I}$ represent deviations from equilibrium. Substituting into (5)–(7) and retaining only linear terms yields the linearized system:

$$\frac{\partial \widetilde{C}}{\partial t} = D_C \Delta \widetilde{C} + \left(r - \frac{2r}{K} C^* - \alpha M^* - \beta I^* + \varepsilon F\right) \widetilde{C} - \alpha C^* \widetilde{M} - \beta C^* \widetilde{I}, \tag{11}$$

$$\frac{\partial \widetilde{M}}{\partial t} = D_M \Delta \widetilde{M} - (\gamma + \rho C^*) \widetilde{M} - \rho M^* \widetilde{C}, \tag{12}$$

$$\frac{\partial \widetilde{I}}{\partial t} = D_I \Delta \widetilde{I} + \delta I^* \widetilde{M} + (\delta M^* - \mu C^*)\,\widetilde{I} - \mu I^* \widetilde{C}. \tag{13}$$

Stability criterion via eigenvalue analysis

Let $\{-\lambda_k\}_{k=0}^{\infty}$ denote the eigenvalues of the Laplace operator Δ on Ω with homogeneous Neumann boundary conditions, with corresponding orthonormal eigenfunctions $\{\phi_k(x)\}$. We expand the perturbations in modal form:

$$\widetilde{C}(x,t) = c_k(t)\phi_k(x), \quad \widetilde{M}(x,t) = m_k(t)\phi_k(x), \quad \widetilde{I}(x,t) = i_k(t)\phi_k(x).$$

Substituting into (11)-(13) yields, for each mode k,

$$\frac{d}{dt}\begin{bmatrix} c_k \\ m_k \\ i_k \end{bmatrix} = (J - \Lambda_k)\begin{bmatrix} c_k \\ m_k \\ i_k \end{bmatrix},$$

where

$$\Lambda_k = \begin{bmatrix} D_C \lambda_k & 0 & 0 \\ 0 & D_M \lambda_k & 0 \\ 0 & 0 & D_I \lambda_k \end{bmatrix},$$

and J is the Jacobian matrix of the reaction terms evaluated at the steady state:

$$J = \begin{bmatrix} r - \frac{2r}{K}C^* - \alpha M^* - \beta I^* + \varepsilon F & -\alpha C^* & -\beta C^* \\ -\rho M^* & -(\gamma + \rho C^*) & 0 \\ -\mu I^* & \delta I^* & \delta M^* - \mu C^* \end{bmatrix}. \tag{14}$$

The matrix $J - \Lambda_k$ determines the growth or decay of perturbations in the k-th spatial mode. The equilibrium (C^*, M^*, I^*) is said to be *locally asymptotically stable* if and only if all eigenvalues of $J - \Lambda_k$ satisfy

$$\Re(\lambda) < 0, \qquad \text{for all } k \geq 0.$$

Since Λ_k has non-negative diagonal entries ($D_C \lambda_k, D_M \lambda_k, D_I \lambda_k \geq 0$), diffusion tends to stabilize the system further by shifting the spectrum of J towards the left half-plane. Therefore, the critical case for stability is the homogeneous mode $k = 0$, for which $\Lambda_0 = 0$.

Thus, the local asymptotic stability of (C^*, M^*, I^*) reduces to the stability of the Jacobian J in (14). Applying the Routh–Hurwitz criterion to the characteristic polynomial

$$\det(\xi I - J) = \xi^3 + a_1 \xi^2 + a_2 \xi + a_3,$$

the following conditions are necessary and sufficient:

$$a_1 > 0, \qquad a_3 > 0, \qquad a_1 a_2 > a_3.$$

Biologically, these conditions ensure that the combined effects of cancer proliferation, melatonin regulation, immune activation, and stress amplification balance in such a way that small pertur-

bations decay over time. Hence, if the Routh–Hurwitz inequalities are satisfied, the equilibrium (C^*, M^*, I^*) is locally asymptotically stable both in the absence and presence of diffusion.

Routh–Hurwitz coefficients and local stability conditions

Jacobian. The Jacobian of the reaction terms at the equilibrium (C^*, M^*, I^*) is given by

$$J = \begin{bmatrix} A & -\alpha C^* & -\beta C^* \\ -\rho M^* & -(\gamma + \rho C^*) & 0 \\ -\mu I^* & \delta I^* & \delta M^* - \mu C^* \end{bmatrix}, \qquad A := r - \frac{2r}{K} C^* - \alpha M^* - \beta I^* + \varepsilon F.$$

Characteristic polynomial. The characteristic polynomial of J is

$$\det(\xi I - J) = \xi^3 + a_1 \xi^2 + a_2 \xi + a_3,$$

with coefficients defined by

$$a_1 = -\operatorname{tr}(J), \qquad a_2 = \sum_{\text{all } 2\times 2 \text{ principal minors}} \det(\cdot), \qquad a_3 = -\det(J).$$

(i) The trace-based coefficient a_1.

$$\begin{aligned} a_1 &= -\big(A - (\gamma + \rho C^*) + (\delta M^* - \mu C^*)\big) = -A + \gamma + \rho C^* - \delta M^* + \mu C^* \\ &= -r + \frac{2r}{K} C^* + \alpha M^* + \beta I^* - \varepsilon F \\ &\quad + \gamma + (\rho + \mu) C^* - \delta M^*. \end{aligned}$$

(ii) The coefficient a_2 (sum of principal minors). For a 3×3 matrix,

$$a_2 = (1,2)\text{-minor} + (1,3)\text{-minor} + (2,3)\text{-minor}.$$

A direct computation gives

$$\begin{aligned} a_2 &= -A(\gamma + \rho C^*) - \alpha \rho C^* M^* + A(\delta M^* - \mu C^*) - \beta \mu C^* I^* \\ &\quad - (\gamma + \rho C^*)(\delta M^* - \mu C^*) \\ &= A\big[(\delta M^* - \mu C^*) - (\gamma + \rho C^*)\big] - \alpha \rho C^* M^* - \beta \mu C^* I^* \\ &\quad - (\gamma + \rho C^*)(\delta M^* - \mu C^*). \end{aligned}$$

(iii) The determinant-based coefficient a_3. Using Laplace expansion, one obtains

$$\begin{aligned} \det(J) = -A(\gamma + \rho C^*)(\delta M^* - \mu C^*) &- \alpha \rho C^* M^* (\delta M^* - \mu C^*) \\ &+ \beta C^* I^* \big(\rho \delta M^* + \mu(\gamma + \rho C^*)\big). \end{aligned}$$

Therefore,

$$a_3 = -\det(J) = A(\gamma + \rho C^*)(\delta M^* - \mu C^*) + \alpha \rho C^* M^* (\delta M^* - \mu C^*) - \beta C^* I^* \big(\rho \delta M^* + \mu(\gamma + \rho C^*)\big).$$

Routh–Hurwitz criterion (reaction part). For the homogeneous mode ($k = 0$), local asymptotic stability requires

$$a_1 > 0, \qquad a_3 > 0, \qquad a_1 a_2 > a_3.$$

For higher modes ($k \geq 1$), the stability matrix is $J - \Lambda_k$, where $\Lambda_k = \text{diag}(D_C \lambda_k, D_M \lambda_k, D_I \lambda_k) \succeq 0$. Since diffusion shifts the spectrum to the left, the most critical case is usually $k = 0$.

Biological interpretation.

- $a_1 > 0$ requires that the overall inhibitory effects (immune suppression, melatonin decay) outweigh the proliferative and stress-amplifying contributions. A sufficiently large γ (melatonin decay) and μC^* (cancer-induced immune suppression) help ensure this balance, provided that δM^* (immune activation by melatonin) does not dominate excessively.
- $a_3 > 0$ strongly depends on the sign of $(\delta M^* - \mu C^*)$. If immune suppression dominates ($\mu C^* > \delta M^*$), the first two terms tend to be negative; stability then relies on the balancing contribution from the last term, which couples β, ρ, μ with I^* and M^*.
- The inequality $a_1 a_2 > a_3$ enforces a mixed balance. In practice, if A (the net proliferation coefficient) is sufficiently reduced (e.g., by high C^* or strong inhibitory effects $\alpha M^*, \beta I^*$, and stress feedback εF), this condition is easier to satisfy.

Effect of diffusion. For each $k \geq 0$, the modal matrix has characteristic polynomial

$$\det(\xi I - (J - \Lambda_k)) = \xi^3 + a_1(k)\xi^2 + a_2(k)\xi + a_3(k),$$

with $a_j(0) = a_j$. As λ_k increases, the diagonal entries of Λ_k grow, shifting the spectrum further left. Thus, if the Routh–Hurwitz conditions are satisfied for $k = 0$, they typically hold for all higher modes as well.

6 Model parameters

In order to simulate the spatiotemporal dynamics of breast cancer progression and its modulation by melatonin and immune interactions, the system of reaction–diffusion equations requires biologically meaningful parameters. Each parameter encapsulates a specific biological process, ranging from intrinsic tumor growth to the effects of melatonin on both cancer and immune components, as well as the tumor-promoting influence of fibroblasts. Careful estimation of these parameters is essential to ensure that the model reflects physiological and clinical realities.

Table 1 summarizes the parameter set employed in this study, with values derived from experimental measurements, clinical studies, and previously validated mathematical models. The tumor growth rate r is based on in vitro and in vivo proliferation studies of breast cancer cells, while the carrying capacity K reflects the maximum achievable cell density in solid tumor tissue. Diffusion coefficients D_C, D_M, and D_I capture the motility of cancer cells, melatonin molecules, and immune cells, respectively, within the tumor microenvironment.

Interaction terms describe regulatory cross-talk among cancer, melatonin, and immune responses. The coefficient α quantifies melatonin's inhibitory action on tumor proliferation, consistent with its known oncostatic role in estrogen receptor-positive breast cancer. Similarly, β represents immune-mediated tumor cell killing, while μ captures cancer-induced immune suppression. Melatonin metabolism and turnover are governed by the decay rate γ and the tumor-associated suppression term ρ, reflecting experimental observations of rapid melatonin clearance and tumor-driven

Table 1. Parameter values used in the reaction–diffusion model of breast cancer dynamics incorporating melatonin–immune interactions

Parameter	Description	Value (units)	Source
r	Intrinsic cancer cell growth rate	3.48×10^{-8} s^{-1}	[17]
D_C	Diffusion coefficient of cancer cells	3.5×10^{-5} cm^2/s (≈ 3.0 mm^2/day)	[18]
D_M	Diffusion coefficient of melatonin	1.0×10^{-9} cm^2/s (≈ 0.086 mm^2/day)	[19]
D_I	Diffusion coefficient of immune cells	1.0×10^{-9} cm^2/s (≈ 0.086 mm^2/day)	[20, 21]
α	Melatonin inhibition of cancer	0.215 (nM^{-1} day^{-1})	[18]
β	Immune killing of cancer	≈ 1.0 (cell^{-1} day^{-1})	[22]
γ	Melatonin decay rate	0.7 h^{-1} (≈ 16.8 day^{-1}); range: 0.5–1.0 h^{-1} (12–24 day^{-1})	[23]
ρ	Cancer-induced melatonin suppression	$\sim 10^{-7}$ (cell^{-1} day^{-1})	[24, 25]
δ	Melatonin-driven immune activation	8.15 (nM^{-1} day^{-1})	[18]
μ	Immune suppression term	0.25 (cell^{-1} day^{-1})	[18]
ε	Fibroblast–cancer interaction	~ 0.1 (day^{-1})	[17, 26]
K	Carrying capacity of tumor cells	10^8–10^9 cells/cm^3	[17]
s	Immune cell source term	$\sim 10^4$ cells/day	[17]
p	Melatonin production rate	5–10 nM/day	[17]

Model parameters compiled from multiple studies on cancer dynamics, melatonin signaling, and immune response interactions

depletion. The stimulatory effect of melatonin on immune activation is modeled by δ, whereas ε accounts for the pro-tumorigenic influence of fibroblasts.

Finally, source terms s and p describe the baseline influx of immune cells into the tumor and the physiological production of melatonin, respectively. In particular, the parameter p is adjusted to reflect the elevated nocturnal melatonin levels reported in blind women, who maintain robust circadian melatonin secretion in the absence of light suppression. This adjustment is critical, as it emphasizes the potential protective role of melatonin in hormone-dependent cancers such as breast cancer.

Overall, the chosen parameter values Table 1 are consistent with data from peer-reviewed studies and provide a biologically informed foundation for the stability analysis and numerical simulations developed in the following sections.

7 Numerical solution via finite differences

Discretization framework

To investigate the spatiotemporal dynamics of breast cancer cells $C(x,t)$, melatonin concentration $M(x,t)$, and immune response $I(x,t)$, the reaction–diffusion system

$$\frac{\partial C}{\partial t} = D_C \Delta C + rC\left(1 - \frac{C}{K}\right) - \alpha MC - \beta IC + \varepsilon FC,$$

$$\frac{\partial M}{\partial t} = D_M \Delta M - \gamma M + p - \rho CM,$$

$$\frac{\partial I}{\partial t} = D_I \Delta I + s + \delta MI - \mu CI,$$

is solved numerically using a finite-difference discretization in both time and space. The domain $\Omega = (0, L)$ is divided into N uniform intervals of size $\Delta x = L/N$, while time is discretized with a step size Δt up to a final time T. The grid points are denoted $x_i = i\Delta x$ for $i = 0, 1, \ldots, N$ and $t^n = n\Delta t$.

Time-Scale Justification: The simulation time intervals (5, 10, and 20 days) were selected to represent short-, medium-, and long-term tumor evolution within physiologically relevant ranges

observed in preclinical and clinical breast cancer studies. These durations correspond to typical cellular proliferation and immune response cycles under in vitro and in vivo conditions, providing a biologically meaningful temporal window for assessing tumor–melatonin–immune interactions. From a mathematical perspective, these time frames also ensure numerical stability and convergence of the finite difference scheme while capturing the essential dynamical transitions of the system.

Spatial approximation

The Laplacian is approximated by the standard second-order central difference operator

$$(\Delta_d U)_i^n = \frac{U_{i-1}^n - 2U_i^n + U_{i+1}^n}{(\Delta x)^2},$$

for $U \in \{C, M, I\}$. Homogeneous Neumann boundary conditions are enforced by ghost-point reflection:

$$U_{-1}^n = U_1^n, \qquad U_{N+1}^n = U_{N-1}^n,$$

which guarantees zero-flux at the boundaries [27, 28].

Temporal discretization: IMEX scheme

To balance stability and computational efficiency, an implicit–explicit (IMEX) Euler scheme is used. Diffusion terms are treated implicitly to remove the parabolic CFL restriction, while nonlinear reaction terms are evaluated explicitly. For each variable, we obtain:

$$\frac{C_i^{n+1} - C_i^n}{\Delta t} = D_C(\Delta_d C^{n+1})_i + R_C(C_i^n, M_i^n, I_i^n),$$

$$\frac{M_i^{n+1} - M_i^n}{\Delta t} = D_M(\Delta_d M^{n+1})_i + R_M(C_i^n, M_i^n),$$

$$\frac{I_i^{n+1} - I_i^n}{\Delta t} = D_I(\Delta_d I^{n+1})_i + R_I(C_i^n, M_i^n, I_i^n),$$

where the reaction operators are

$$R_C = rC\left(1 - \frac{C}{K}\right) - \alpha MC - \beta IC + \varepsilon FC,$$

$$R_M = -\gamma M + p - \rho CM,$$

$$R_I = s + \delta MI - \mu CI.$$

Linear systems for implicit step

For each species $U \in \{C, M, I\}$, the implicit step leads to a tridiagonal system:

$$-\kappa_U U_{i-1}^{n+1} + (1 + 2\kappa_U) U_i^{n+1} - \kappa_U U_{i+1}^{n+1} = U_i^n + \Delta t\, R_{U,i}^n, \qquad i = 1, \ldots, N-1,$$

with $\kappa_U = D_U \Delta t / (\Delta x)^2$. At the boundaries, homogeneous Neumann conditions yield

$$(1 + \kappa_U) U_0^{n+1} - \kappa_U U_1^{n+1} = U_0^n + \Delta t\, R_{U,0}^n,$$

$$-\kappa_U \, U_{N-1}^{n+1} + (1 + \kappa_U) \, U_N^{n+1} = U_N^n + \Delta t \, R_{U,N}^n.$$

Each tridiagonal system is solved efficiently using the Thomas algorithm with $\mathcal{O}(N)$ complexity. The numerical procedure begins with the initialization of all model parameters, including $r, K, \alpha, \beta, \gamma,$ $\rho, \delta, \mu, \varepsilon, D_C, D_M, D_I, s,$ and p, as provided in Table 1. The spatial domain is discretized by defining the grid points $x_i = i\Delta x$ for $i = 0, \ldots, N$, while the temporal domain is partitioned into uniform steps $t^n = n\Delta t$. Appropriate initial conditions are prescribed, consisting of a small localized tumor density C^0, baseline melatonin concentration M^0, and an initial immune cell density I^0. At each time step, the nonlinear reaction terms $R_C, R_M,$ and R_I are evaluated using the current solution values (C^n, M^n, I^n), and the resulting systems of tridiagonal equations are solved to update $C^{n+1}, M^{n+1},$ and I^{n+1}. To preserve biological realism, non-negativity is enforced by projecting negative values onto zero. This procedure is repeated iteratively until the final time $t = T$ is reached, after which the time evolution and spatial distributions of the variables are analyzed and visualized.

Computational implementation. All numerical simulations were performed using MATLAB R2024a. The finite difference scheme was implemented within MATLAB's numerical computation environment to ensure high precision and stability in solving the coupled reaction–diffusion equations.

Immune profile: mathematical and biological interpretation

The spatial–temporal evolution of immune cell density $I(x, t)$ is illustrated in Figure 5. Mathematically, the immune component satisfies a reaction–diffusion equation characterized by both local proliferation and tumor-induced suppression terms.
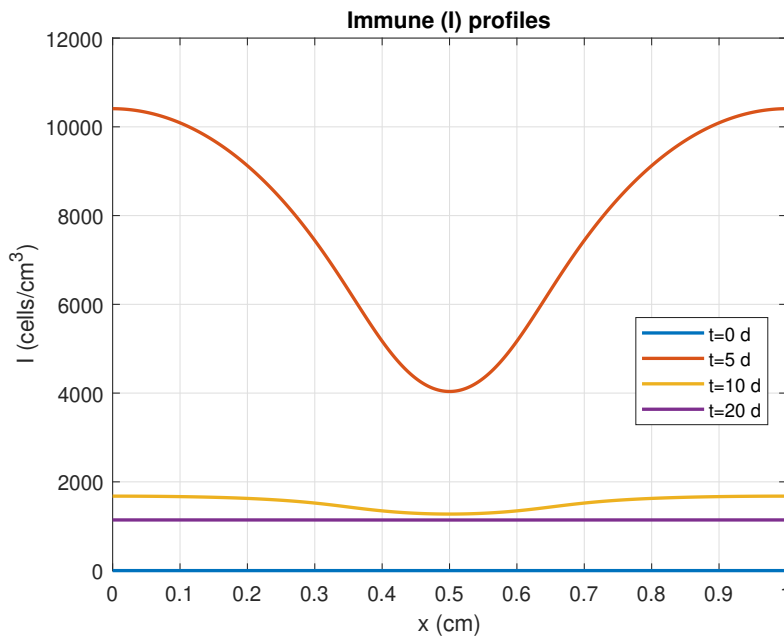

Figure 5. Immune cell density $I(x, t)$ profiles at different times ($t = 0, 5, 10, 20$ days). The spatial distribution shows an initial uniform baseline, followed by a pronounced dip at the tumor core ($x = 0.5$) due to cancer-induced immunosuppression. Over time, immune density stabilizes at reduced levels across the domain, consistent with chronic tumor-driven suppression of host immunity

Initially, the distribution is spatially uniform ($t = 0$), indicating a steady immune baseline

throughout the domain. As time progresses ($t = 5$ days), a significant decrease in immune cell concentration is observed at the tumor core ($x = 0.5$), reflecting the strong local inhibition caused by cancer–immune interactions represented by the term $-\mu CI$. Over subsequent time intervals ($t = 10, 20$ days), the immune profile gradually stabilizes at lower levels, suggesting a diffusion-driven homogenization of the suppressed immune field. Biologically, this pattern corresponds to chronic immunosuppression within the tumor microenvironment. Cancer cells locally inhibit immune activity, resulting in a central depletion of immune cells, while peripheral regions maintain slightly higher immune densities. The eventual stabilization at reduced levels indicates a sustained balance between immune recruitment and tumor-mediated suppression, consistent with the progression toward immune exhaustion in advanced cancer dynamics.

Melatonin profiles: mathematical and biological interpretation

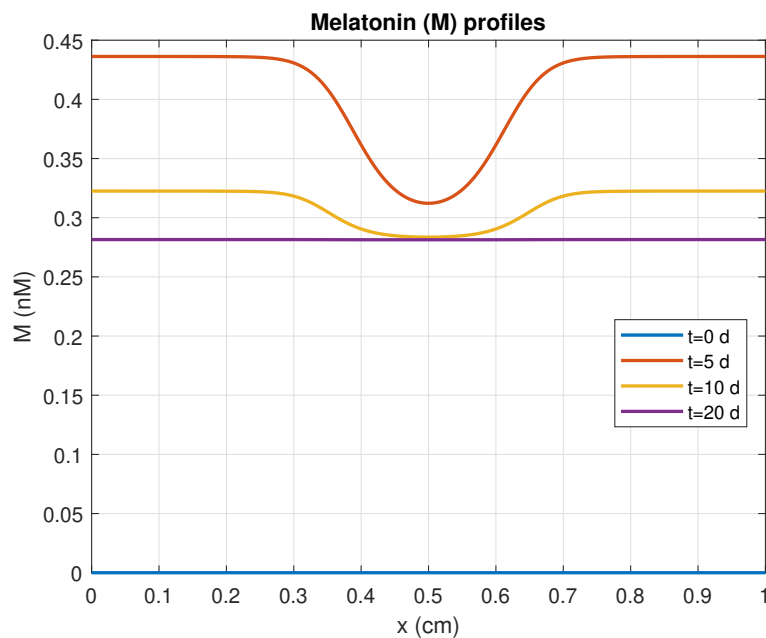The spatial–temporal evolution of melatonin $M(x, t)$ is illustrated in Figure 6.

Figure 6. Melatonin concentration $M(x, t)$ profiles at different times ($t = 0, 5, 10, 20$ days). Initially, melatonin is uniform across the spatial domain. As tumor growth progresses, a pronounced dip in melatonin levels emerges around the tumor core ($x = 0.5$), reflecting cancer-induced melatonin suppression. Over time, the baseline melatonin concentration decreases globally, consistent with chronic tumor burden and stress-related circadian disruption

Mathematical interpretation. Initially ($t = 0$), melatonin is uniformly distributed across the spatial domain. As time progresses, the governing reaction–diffusion equation

$$\frac{\partial M}{\partial t} = D_M \Delta M - \gamma M + p - \rho CM$$

induces spatial heterogeneity. The term $-\rho CM$, representing cancer-induced melatonin suppression, dominates near the tumor core, producing a localized dip around $x = 0.5$. Over time, the interplay among diffusion ($D_M \Delta M$), natural decay ($-\gamma M$), and production (p) drives melatonin toward a lower steady-state distribution. By $t = 20$ days, the profile flattens at a suppressed level, reflecting convergence to a stable equilibrium influenced by tumor burden and metabolic

depletion.

Biological interpretation. As shown in Figure 6, the simulated profiles reveal that melatonin, initially sufficient to sustain antioxidant and hormonal regulation, becomes depleted in the tumor microenvironment due to cancer-induced suppression. The central dip corresponds to the tumor region, where cancer cells most actively inhibit or consume melatonin. This decline weakens melatonin's protective roles, such as reducing oxidative stress and modulating estrogen signaling, thereby facilitating tumor progression. At later stages, melatonin remains chronically suppressed throughout the tissue, indicating systemic depletion under persistent tumor stress. This observation aligns with clinical evidence showing that reduced melatonin levels are associated with poor prognosis in breast cancer, while persistently high melatonin concentrations (as observed in blind women) mitigate tumor progression by preserving antioxidant and immunomodulatory defenses.

Tumor density dynamics: mathematical and biological interpretation

Tumor density $C(x, t)$ is figured out for various values of time scales in Figure 7.
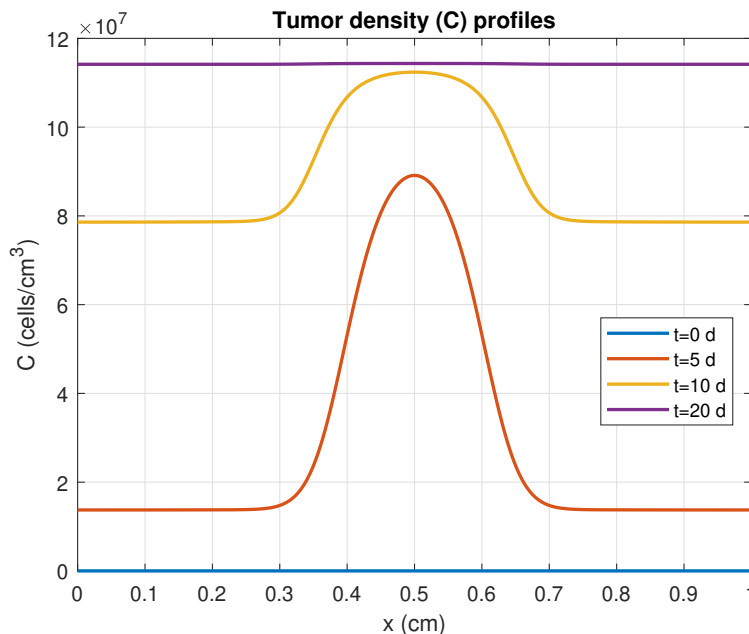

Figure 7. Tumor density $C(x, t)$ profiles at different times ($t = 0, 5, 10, 20$ days). The simulation shows localized tumor proliferation around the center of the domain ($x = 0.5$ cm), with growth saturating as the carrying capacity K is approached

Mathematical perspective: Figure 7 illustrates the spatiotemporal evolution of tumor density $C(x, t)$ obtained from the finite difference scheme. Initially ($t = 0$), the distribution is uniform and near zero, reflecting the prescribed small perturbation. By $t = 5$ days, the tumor exhibits exponential growth localized around the center of the spatial domain ($x = 0.5$ cm), consistent with the logistic growth term $rC(1 - C/K)$ in the governing equations. The influence of diffusion ($D_C \Delta C$) leads to gradual spatial spreading, but the proliferation term dominates, driving the tumor toward the carrying capacity K. At later times ($t = 10, 20$ days), the tumor density approaches saturation, and the growth stabilizes as $C(x, t) \to K$, which mathematically confirms the existence of a biologically relevant steady state.

Biological perspective: From a biological standpoint, the simulations capture the hallmark

dynamics of tumor progression. In the early phase, cancer cells proliferate rapidly, forming a dense cluster around the tumor core. As time progresses, growth is counterbalanced by environmental limitations (e.g., nutrient depletion, space constraints), reflected in the carrying capacity K. The interaction terms with melatonin and immune cells ($-\alpha MC$, $-\beta IC$) reduce effective proliferation, but under stress-induced circadian disruption, their protective influence is weakened, enabling the tumor to expand until near-saturation. The long-term plateau in tumor density suggests that without sufficient melatonin regulation or immune clearance, the tumor achieves a quasi-stable high-density state, aligning with biological observations in aggressive tumor growth under chronic stress conditions.

Spatio–temporal dynamics of the cancer–melatonin–immune system

Numerical simulations of the reaction–diffusion breast cancer–melatonin–immune model, calibrated with biologically grounded parameters Table 1, reveal the spatio–temporal interplay among tumor density, melatonin concentration, and immune activity. As illustrated in Figure 8, at early times (e.g., $t = 1.5$–5 days), the tumor exhibits localized growth with a pronounced peak at the center, while melatonin levels drop sharply in the tumor core, reflecting cancer–induced suppression. Concurrently, immune cell density shows a dip in the same region, consistent with localized immunosuppression. As time progresses ($t = 6$–10.5 days), the tumor mass expands towards the carrying capacity, melatonin declines further, and immune density decreases substantially in the tumor zone, highlighting the imbalance between tumor proliferation and host defenses. At later stages ($t = 17.5$–20 days), the system approaches a quasi–steady state: cancer cells saturate near the carrying capacity, melatonin stabilizes at suppressed levels, and immune activity remains diminished. This temporal progression demonstrates the destabilizing effect of stress–induced cancer amplification and melatonin depletion, while also emphasizing the protective role of high baseline melatonin (as observed in blind women) in counteracting tumor growth.
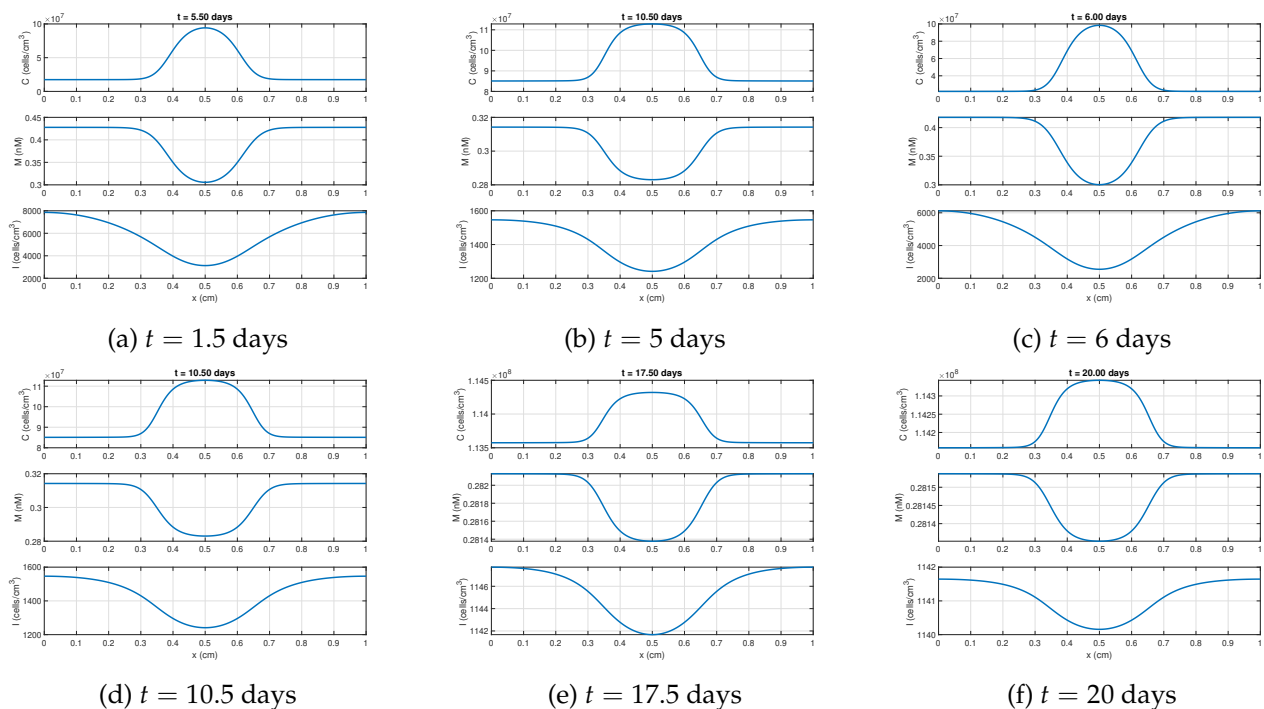

Figure 8. Time evolution of tumor density $C(x,t)$, melatonin concentration $M(x,t)$, and immune response $I(x,t)$ at selected times. Subfigures (a)–(f) correspond to different time points, showing the coupled spatio-temporal dynamics

8 Conclusion

In this work, we proposed and rigorously analyzed a nonlinear reaction–diffusion model to investigate the complex interplay between breast cancer dynamics, melatonin regulation, and immune responses, with a particular emphasis on blind women whose persistently elevated melatonin levels confer distinct biological advantages. The model was constructed by integrating key biological processes, including tumor logistic proliferation, melatonin-driven hormonal modulation, oxidative stress suppression, and immune-mediated cytotoxicity, into a mathematical framework that accounts for spatial heterogeneity and temporal evolution. From a theoretical perspective, we established the existence and uniqueness of weak solutions using Galerkin approximations, energy estimates, and compactness arguments within Sobolev spaces, thereby ensuring the mathematical validity of the proposed framework. Stability analysis was carried out through linearization and eigenvalue methods, demonstrating that the long-term tumor behavior depends critically on the balance between proliferation rates and melatonin–immune suppression terms. In particular, we showed that sufficient melatonin production, such as that observed in blind populations, can shift the system towards stable equilibria that limit or even suppress tumor expansion, whereas impaired melatonin regulation leads to unstable dynamics favoring tumor persistence.

Numerical simulations performed via implicit–explicit finite difference schemes further substantiated these analytical results, illustrating the spatio–temporal progression of tumor density, melatonin concentration, and immune activity. The simulations highlighted the role of melatonin in preserving circadian integrity, reducing estrogen-driven proliferation, and enhancing immune cell activation, while also revealing the detrimental impact of cancer-induced melatonin suppression. Biologically, our findings align with epidemiological studies reporting a markedly reduced incidence of hormone-dependent cancers in blind individuals, underscoring the protective role of melatonin against circadian disruption and tumor growth.

Moreover, the model emphasizes that stress-induced circadian misalignment exacerbates cancer progression by weakening melatonin's antioxidative and immunoregulatory functions, thereby offering new insights into the pathophysiological links between stress, hormonal imbalance, and cancer. Taken together, this study demonstrates the power of combining biological insights with mathematical modeling to provide a mechanistic understanding of cancer dynamics, and it supports the consideration of melatonin supplementation or circadian-based therapeutic strategies as potential adjunctive approaches in breast cancer prevention and treatment, particularly for populations at high risk of circadian disruption, such as shift workers. Beyond breast cancer, the presented framework may be extended to other hormone-sensitive or stress-related cancers, offering a versatile tool for exploring how biological rhythms intersect with tumorigenesis and guiding future interdisciplinary research at the interface of oncology, endocrinology, and applied mathematics.

9 Potential implications

The present reaction–diffusion model offers broader insight into how circadian and hormonal regulation influence cancer dynamics. Beyond breast cancer, this framework could be extended to other hormone-dependent or stress-related malignancies. By integrating melatonin's effects on immune activity and oxidative balance, the model provides a foundation for exploring chronotherapy and personalized treatment strategies.

Moreover, it encourages future interdisciplinary research linking circadian biology, oncology, and applied mathematics.

Declarations

Use of AI tools

The authors declare that they have not used Artificial Intelligence (AI) tools in the creation of this article.

List of abbreviations

ASR: Age-Standardized Rate
CAT: Catalase
CTL: Cytotoxic T Lymphocyte
ER: Estrogen Receptor
GPx: Glutathione Peroxidase
IARC: International Agency for Research on Cancer
IFN-γ: Interferon-Gamma
IL-10: Interleukin-10
NK: Natural Killer (Cell)
NF-κB: Nuclear Factor Kappa-Light-Chain-Enhancer of Activated B Cells
Nrf2: Nuclear Factor Erythroid 2–Related Factor 2
ODE: Ordinary Differential Equation
PDE: Partial Differential Equation
ROS: Reactive Oxygen Species
SOD: Superoxide Dismutase
TAM: Tumor-Associated Macrophage
TGF-β: Transforming Growth Factor-Beta
Treg: Regulatory T Cell
VEGF: Vascular Endothelial Growth Factor

Data availability statement

All data generated or analyzed during this study are included in this article.

Ethical approval

The authors state that this research adheres to the ethical standards. This research does not involve either human participants or animals.

Consent for publication

Not applicable

Conflicts of interest

The authors declare that they have no conflict of interest.

Funding

No funding was received to support this study.

Author's contributions

A.E.: Conceptualization, Methodology, Software, Formal Analysis, Visualization, Writing – Original Draft Preparation. F.A.: Supervision, Validation, Writing – Review & Editing. Both authors

discussed the results, contributed to the interpretation of findings, and approved the final version of the manuscript.

References

[1] World Health Organization, International Agency for Research on Cancer (IARC). [https://iarc.who.int/], [Accessed: 12/09/2025]

[2] World Health Organization, International Agency for Research on Cancer (IARC), Cancer Over Time: Cohort data - Populations=792, Sexes=2. *GLOBOCAN,* (2025). [https://gco.iarc.fr/overtime/en/dataviz/cohorts?populations=792&sexes=2], [Accessed: 12/09/2025]

[3] Yi, Y.J., Tang, H., Pi, P.L., Zhang, H.W., Du, S.Y., Ge, W.Y. et al. Melatonin in cancer biology: Pathways, derivatives, and the promise of targeted delivery. *Drug Metabolism Reviews,* 56(1), 62-79, (2024). [CrossRef]

[4] Bayrakçeken, E., Yaralı, S. and Alkan, Ö. Identify risk factors affecting participation of Turkish women in mammography screening for breast cancer prevention. *Breast Cancer Research and Treatment,* 205, 487-495, (2024). [CrossRef]

[5] Bray, F., Laversanne, M., Sung, H., Ferlay, J., Siegel, R.L., Soerjomataram, I. and Jemal, A. Global cancer statistics 2022: GLOBOCAN estimates of incidence and mortality worldwide for 36 cancers in 185 countries. *CA: A Cancer Journal for Clinicians,* 74(3), 229-263, (2024). [CrossRef]

[6] Joshi, H., Yavuz, M. and Stamova, I. Analysis of the disturbance effect in intracellular calcium dynamic on fibroblast cells with an exponential kernel law. *Bulletin of Biomathematics,* 1(1), 24-39, (2023). [CrossRef]

[7] Duffy, S.W., Vulkan, D., Cuckle, H., Parmar, D., Sheikh, S., Smith, R.A. et al. Effect of mammographic screening from age 40 years on breast cancer mortality (UK Age trial): final results of a randomised, controlled trial. *The Lancet Oncology,* 21(9), 1165-1172, (2020). [CrossRef]

[8] Calvo, J.R. and Maldonado, M.D. Immunoregulatory properties of melatonin in the humoral immune system: A narrative review. *Immunology Letters,* 269, 106901, (2024). [CrossRef]

[9] Koul, A.M., Shafi, T., Anwar, I., Banday, M., Iqra, S., Gull, A. et al. Melatonin and immune modulation. In *Melatonin: A Ubiquitous Pleiotropic Molecule* (pp. 163-185). Elsevier, New York, USA: Academic Press, (2024). [CrossRef]

[10] Motehaver, A.N., Sheida, F., Javadinia, S.A., Behzadi, B., Afshar, S., Khezrian, A. et al. Melatonin and breast cancer: A review article. *Chonnam Medical Journal,* 61(2), 63-74, (2025). [CrossRef]

[11] Yu, Z.Y., Peng, R.Y., Cheng, N., Wang, R.T., Nan, M.D., Milazzo, S. et al. Melatonin in cancer treatment. *Cochrane Database of Systematic Reviews,* 4, CD010145, (2025). [CrossRef]

[12] de Pillis, L.G., Radunskaya, A.E. and Wiseman, C.L. A validated mathematical model of cell-mediated immune response to tumor growth. *Cancer Research,* 65(17), 7950-7958, (2005). [CrossRef]

[13] Ekmekcioglu, C. Melatonin receptors in humans: Biological role and clinical relevance. *Biomedicine & Pharmacotherapy,* 60(3), 97-108, (2006). [CrossRef]

[14] Pukkala, E., Ojamo, M., Rudanko, S.L., Stevens, R.G. and Verkasalo, P.K. Does incidence of breast cancer and prostate cancer decrease with increasing degree of visual impairment. *Cancer Causes & Control,* 17, 573–576, (2006). [CrossRef]

[15] Minella, C., Coliat, P., Amé, S., Neuberger, K., Stora, A., Mathelin, C. and Reix, N. Protective role of melatonin in breast cancer: what we can learn from women with blindness. *Cancer Causes & Control,* 33, 1-13, (2022). [CrossRef]

[16] Ucar, S., Koca, İ., Özdemir, N. and İnci, T. A stochastic approach to tumor modeling incorporating macrophages. *Bulletin of Biomathematics,* 2(2), 162-181, (2024). [CrossRef]

[17] Lee, J. and Kim, E. Ordinary differential equation model of cancer-associated fibroblast heterogeneity predicts treatment outcomes. *Systems Biology and Applications,* 11, 96, (2025). [CrossRef]

[18] Andasari, V., Gerisch, A., South, A.P. and Chaplain, M.A. J. Mathematical modeling of cancer cell invasion of tissue: Development of an *in silico* organotypic assay. *bioRxiv,* 1-19, (2025). [CrossRef]

[19] Roma-Rodrigues, C., Mendes, R., Baptista, P.V. and Fernandes, A.R. Targeting tumor microenvironment for cancer therapy. *International Journal of Molecular Sciences,* 20(4), 840, (2019). [CrossRef]

[20] Carrillo-Vico, A., Guerrero, J.M., Lardone, P.J. and Reiter, R.J. A review of the multiple actions of melatonin on the immune system. *Endocrine,* 27, 189-200, (2005). [CrossRef]

[21] Kubatka, P., Zubor, P., Busselberg, D., Kwon, T.K., Adamek, M., Petrovic, D. et al. Melatonin and breast cancer: Evidences from preclinical and human studies. *Critical Reviews in Oncology/Hematology,* 122, 133-143, (2018). [CrossRef]

[22] Storey, K.M., Lawler, S.E. and Jackson, T.L. Modeling oncolytic viral therapy, immune checkpoint inhibition, and the complex dynamics of innate and adaptive immunity in glioblastoma treatment. *Frontiers in Physiology,* 11, 151, (2020). [CrossRef]

[23] Eyduran, Ş.P., Çolak, A.M., Berk, S.K., Sakaldaş, M., Şen, F. and Gundogdu, M. Reducing respiration rate and increasing chemical stability of mulberry fruits by using postharvest putrescine and melatonin. *BMC Plant Biology,* 25, 431, (2025). [CrossRef]

[24] Talib, W.H., Alsayed, A.R., Abuawad, A., Daoud, S. and Mahmod, A.I. Melatonin in cancer treatment: current knowledge and future opportunities. *Molecules,* 26(9), 2506, (2021). [CrossRef]

[25] Xu, C., Zhou, J., Li, F. and Wang, H. Melatonin suppression in tumor-bearing models: Mechanisms linking circadian disruption, oxidative stress, and immune dysfunction. *Frontiers in Endocrinology,* 13, 890457, (2022). [CrossRef]

[26] Giangreco, G., Rullan, A., Naito, Y., Biswas, D., Liu, Y.H., Hooper, S. et al. Cancer cell–Fibroblast crosstalk via HB-EGF, EGFR, and MAPK signaling promotes the expression of macrophage chemo-attractants in squamous cell carcinoma. *IScience,* 27(9), 110635, (2024). [CrossRef]

[27] Enver, A. and Ayaz, F. Mathematical modeling of stress-induced type 2 diabetes and atherosclerosis: Numerical methods and stability analysis. *Results in Nonlinear Analysis,* 8(1), 204-225, (2025). [CrossRef]

[28] Enver, A., Ayaz, F. and Yalçınkaya, D.E. A multiscale coupled reaction-diffusion model of

amyloid-beta and tau pathology in Alzheimer's disease. *Journal of Nonlinear Modeling and Analysis*, 7(5), 1940-1964, (2025). [CrossRef]